Mirabamides A–D, Depsipeptides from the Sponge *Siliquariaspongia mirabilis* That Inhibit HIV-1 Fusion

Alberto Plaza,[†] Elena Gustchina,[‡] Heather L. Baker,[†] Michelle Kelly,[§] and Carole A. Bewley*[,†]

Laboratory of Bioorganic Chemistry, National Institute of Diabetes and Digestive and Kidney Diseases, National Institutes of Health, Bethesda, Maryland 20892-0820, Laboratory of Chemical Physics, National Institute of Diabetes and Digestive and Kidney Diseases, National Institutes of Health, Bethesda, Maryland 20892-0820, and National Centre for Aquatic Biodiversity and Biosecurity, National Institute of Water and Atmospheric Research, Newmarket, Auckland, New Zealand

Received June 26, 2007

Four new cyclic depsipeptides termed mirabamides A–D (**1**–**4**) have been isolated from the marine sponge *Siliquariaspongia mirabilis* and shown to potently inhibit HIV-1 fusion. Their structures were elucidated by NMR and ESIMS, and absolute stereochemistry of the amino acids was determined using advanced Marfey's methods and NMR. Mirabamides contain two new entities, including 4-chlorohomoproline in **1**–**3** and an unusual glycosylated amino acid, β-methoxytyrosine 4′-*O*-α-L-rhamnopyranoside (in **1**, **2**, and **4**), along with a rare N-terminal aliphatic hydroxy acid. These elements proved to be useful for anti-HIV structure–activity relationship studies. Mirabamide A inhibited HIV-1 in neutralization and fusion assays with IC_{50} values between 40 and 140 nM, as did mirabamides C and D (IC_{50} values between 140 nM and 1.3 μM for **3** and 190 nM and 3.9 μM for **4**), indicating that these peptides can act at the early stages of HIV-1 entry. The potent activity of depsipeptides containing the glycosylated β-OMe Tyr unit demonstrates that β-OMe Tyr itself is not critical for activity. Mirabamides A–C inhibited the growth of *B. subtilis* and *C. albicans* at 1–5 μg/disk in disk diffusion assays.

Marine organisms have proven to be an extremely rich source of structurally diverse bioactive natural products. Indeed, many marine natural products or their synthetic derivatives are currently in clinical and advanced preclinical trials.[1] In terms of chemical diversity, an exceptionally prolific group of sponges include the lithistid demosponges, which may in part be due to the biosynthetic capacity of the bacteria that they host.[2] Peptides isolated from lithistid demosponges of the family Thonellidae commonly contain unusual amino acids and exhibit potent biological activities. Just a few examples include the highly cytotoxic polytheonamides,[3] HIV inhibitory papuamides,[4] antibacterial nagahamide,[5] antifungal theonegramide,[6] and protease inhibitor miraziridine.[7] In our ongoing studies of natural products with anti-HIV activity, we have identified an aqueous extract of the marine sponge *Siliquariaspongia mirabilis* (de Laubenfels, 1954) (Lithistid Demospongiae: family Theonellidae), collected from Chuuk Lagoon in the Federated States of Micronesia, that shows significant inhibition of HIV-1 at 100 μg/mL as well as antimicrobial activity toward *C. albicans* and *B. subtilis*. Preliminary analysis of the NMR and LC-MS data suggested the presence of new chlorinated, glycosylated depsipeptides. Bioassay-guided fractionation led to the isolation of four new depsipeptides, termed mirabamides A–D (**1**–**4**), along with the known aurantosides A and B.[8] Their structures were elucidated by extensive spectroscopic methods including 1D (^{1}H and ^{13}C) and 2D NMR experiments (DQF-COSY, HOHAHA, HMBC, HSQC, and ROESY) as well as ESIMS analysis.

Results and Discussion

The crude aqueous extract of *S. mirabillis* was partitioned with *n*-BuOH–H_2O. Chromatography of the BuOH extract over Sephadex LH-20 followed by C_{18} reversed-phase HPLC yielded compounds **1**–**4**. The molecular formula of **1** was determined as $C_{72}H_{114}ClN_{13}O_{25}$ on the basis of the HRESIMS (*m/z* 1596.7753 $[M + H]^+$, calcd for $C_{72}H_{115}ClN_{13}O_{25}$, 1596.7816) and NMR data (see Table 1). The isotopic distribution of the ions $[M + H]^+$, 3:1, at *m/z* 1596 and 1598 clearly indicated the presence of chlorine. Although compound **1** displayed a single peak in the HRESIMS, the ^{1}H and ^{13}C NMR spectra in MeOH-d_4 exhibited many doubled or tripled signals. This led us to speculate that the sample contained multiple isomers or was undergoing conformational exchange that is slow on the NMR time scale. By recording ^{1}H NMR spectra in a mixture of 5:1 CD_3CN–H_2O at 298 K using water suppression, we found the latter to be true for MeOH because a well-resolved single spectrum was obtained in acetonitrile–water.

The ^{1}H NMR spectrum of **1** exhibited signals characteristic of a peptide containing numerous aliphatic and oxygenated residues including nine exchangeable NH resonances between δ 7.00 and 9.2, one methyl amide signal at δ 3.04 (3H, s), and seven signals corresponding to eight methyl doublets at δ 1.41 (3H, d, J = 7.2 Hz), 1.24 (3H, d, J = 6.3 Hz), 1.14 (6H, d, J = 6.3 Hz), 1.11 (3H, d, J = 6.2 Hz), 1.00 (3H, d, J = 6.8 Hz), 0.95 (3H, d, J = 6.3 Hz), 0.78 (3H, d, J = 6.3 Hz), and 0.36 (3H, d, J = 5.9 Hz). Additionally, the ^{1}H NMR spectrum showed a signal corresponding to an anomeric proton at δ 5.40 (1H, br s) and signals characteristic of a *para*-substituted phenyl ring at δ 7.32 (2H, dd, J = 8.2, 1.2 Hz) and 7.01 (2H, dd, J = 8.2, 1.2 Hz). The HSQC spectrum of **1** clearly showed that the 13 proton signals at δ 3.80–5.35 were correlated to 11 carbons at δ 43.0–64.5 (nine α-methines and two α-methylenes), suggesting the occurrence of 11 amino acid residues (see Table 1). This evidence in combination with 2D-HOHAHA, COSY, and HMBC correlations allowed us to establish the presence of the amino acid residues β-methoxytyrosine (β-OMeTyr), *N*-methylthreonine (*N*MeThr), alanine, two glycines, 3-methoxyalanine (3-OMeAla), 3-hydroxyleucine (3-OHLeu), 3,4-dimethylglutamine (3,4-DiMeGln), 2,3-diaminobutanoic acid (Dab), threonine, and the sugar unit α-rhamnose (see Table 1). Additional evidence of the presence of an unusual rhamnose residue was obtained from ESIMS/MS experiments. The spectrum of the major ion peak at *m/z* 1597 displayed one daughter ion at *m/z* 1451 $[M + H - 146]^+$ ascribable to the loss of a deoxyhexose unit, corroborating the NMR results.

A spin system starting from an α-methine group (δ_H 4.99, δ_C 50.1) and comprising sequential β-CH_2 (δ_H 2.48, 2.23, δ_C 33.3),

* To whom correspondence should be addressed. Tel: (301) 594-5187. Fax: (301) 402-0008. E-mail: caroleb@mail.nih.gov.
[†] Laboratory of Bioorganic Chemistry, NIDDK, National Institutes of Health.
[‡] Laboratory of Chemical Physics, NIDDK, National Institutes of Health.
[§] National Institute of Water and Atmospheric Research.

10.1021/np070306k CCC: $37.00
Published on Web 10/27/2007

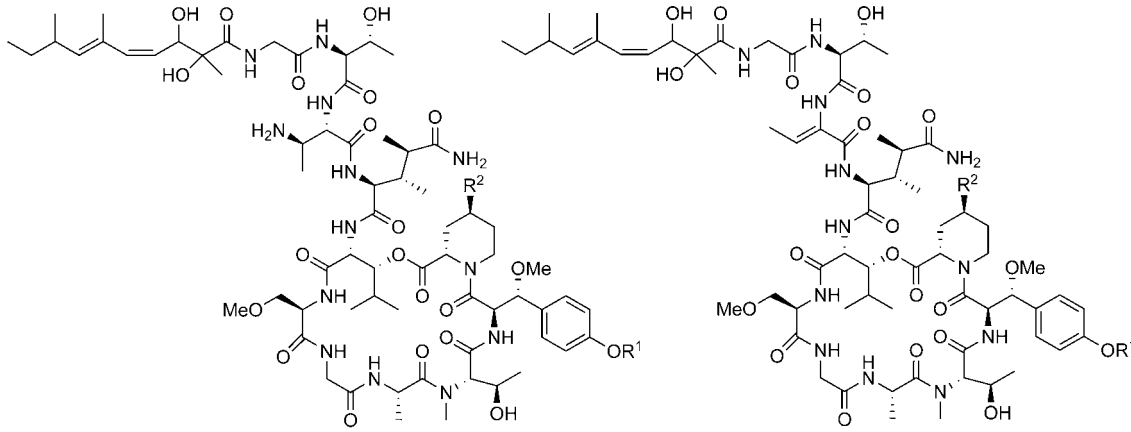

1 R^1 = 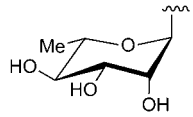 R^2 = Cl

2 R^1 = 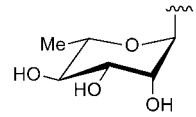 R^2 = Cl

3 R^1 = H R^2 = Cl

4 R^1 = 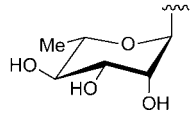 R^2 = H

5 R^1 = H R^2 = H

γ-CHCl (δ_H 4.52, δ_C 56.4), δ-CH_2 (δ_H 1.91, δ_C 33.1), and ε-CH_2N groups (δ_H 4.06, 3.51, δ_C 39.0) was obtained from 2D-HOHAHA, COSY, and HSQC spectra. Evidence that this spin system belonged to a 4-chlorohomoproline (ClHpr) residue came from HMBC correlations between the proton at δ 4.99 (H-2_{ClHpr}) and the carbon resonances at δ 171.1 (C-1_{ClHpr}), 56.4 (C-4_{ClHpr}), and 39.0 (C-6_{ClHpr}). To our knowledge, this is the first occurrence of a chlorinated homoproline in a marine natural product. The presence of 2,3-dihydroxy-2,6,8-trimethyldecadienoic acid (Dhtda) was deduced as follows. The HSQC spectrum contained cross-peaks at δ 125.2, 138.8, and 139.6 corresponding to three olefinic carbons. COSY and 2D-HOHAHA experiments established the presence of two spin systems bearing these olefinic carbons. Long-range correlations from the methyl olefinic protons at δ 1.74 (Me-6_{Dhtda}) to the carbon resonances at δ 131.9 (C-6_{Dhtda}), 138.8 (C-5_{Dhtda}), and 139.6 (C-7_{Dhtda}) connected these two spin systems. Finally, the complete structure of the Dhtda residue was assigned from additional HMBC correlations between the methyl signal at δ 1.17 (Me-2_{Dhtda}) and the carbon resonances at δ 178.5 (C-1_{Dhtda}), 78.8 (C-2_{Dhtda}), and 72.7 (C-3_{Dhtda}) and between the secondary oxygenated proton at δ 4.78 (H-3_{Dhtda}) and the carbon resonances at δ 178.5 (C-1_{Dhtda}) and 125.5 (C-4_{Dhtda}). The *Z* geometry of the $C4_{Dhtda}$–C-5_{Dhtda} double bond was indicated by the large coupling constant (12.3 Hz) between H-5_{Dhtda} and H-4_{Dhtda}. Strong ROESY correlations between Me-6_{Dhtda} (δ 1.74) and H-8_{Dhtda} (δ 2.32) and between H-5_{Dhtda} (δ 6.11) and H-7_{Dhtda} (δ 5.20) suggested an *E* configuration for the olefinic C6–C7.

The downfield chemical shift of the 3-OHLeu β-oxymethine proton at δ 5.17 suggested an ester linkage at this position, which was confirmed by an HMBC correlation between the β-proton of 3-OHLeu and the carbonyl carbon of ClHpr (δ 171.1). Moreover, HMBC correlations from α-protons to carbonyl carbons of adjacent amino acid residues allowed us to establish the connectivity of all amino acids. The connection of Dhtda to the N-terminal Gly2 was established through long-range correlations between the methylene signals at δ 4.04 and 3.80 (H-$2b_{Gly2}$) and the carbonyl resonance at δ 178.5 (C-1_{Ala}). Finally, unambiguous determination of the unusual linkage position of the α-rhamnose unit to the β-methoxytyrosine residue was obtained from an HMBC correlation between the anomeric proton at δ 5.41 and the carbon resonance at δ 157.3 (C-$4'_{\beta\text{-OMeTyr}}$). Although there are just a few reports of glycopeptides isolated from marine organisms,[6,9] to our knowledge this is the first report of a glycosylated tyrosine residue present in a marine natural product. In fact, the occurrence of a tyrosine residue glycosylated at the *para* position has been reported only in the glycopeptide antibiotics mannopeptimycins, isolated from *Streptomyces hygroscopicus*.[10]

Further evidence supporting the peptide sequence of **1** was obtained from the ESIMS/MS spectrum. The daughter ion spectrum of the major ion at *m/z* 1597 $[M + H]^+$ displayed fragment ions at *m/z* 1096 $[M + H - Dhtda - Gly2 - Thr - Dab - NH_3]^+$, *m/z* 957 $[M + H - Dhtda - Gly2 - Thr - Dab - DiMeGln]^+$, and *m/z* 900 $[M + H - Dhtda - Gly2 - Thr - Dab - DiMeGln - Gly1]^+$. This fragmentation pattern was in complete agreement with the NMR results.

At this point, it was evident that the amino acid sequence of **1** resembles that of papuamide A (**5**), only differing by the occurrence of the novel 4-chlorohomoproline and β-methoxytyrosine 4′-*O*-α-L-rhamnopyranoside residues. Papuamide A was previously isolated from extracts of *T. mirabilis* and *T. swinhoei* collected in Papua New Guinea.[4]

The absolute configurations of L-*N*MeThr, L-Thr, L-Ala, D-3-OMeAla, and (2*R*,3*R*)-3-hydroxyleucine residues were assigned by chromatographic comparison of the acid hydrolysate of **1** (5 N HCl, 90 °C, 16 h) with appropriate amino acid standards by LC-MS after derivatizing with L/D-FDLA (1-fluoro-2,4-dinitrophenyl-5-L/D-leucinamide).[11] Comparison by LC-MS of the L/D-FDLA derivatives of 3,4-DiMeGln and Dab of **1** with those derivatives from the hydrolysate of an authentic sample of papuamide A showed that DiMeGln and Dab residues have the same configuration in both peptides. Thus, their configurations were established as (3*S*,4*R*)-dimethyl-L-glutamine and (2*S*,3*R*)-diaminobutanoic acid. The absolute configuration of C-2 of ClHpr was determined to be L by the advanced Marfey's method[11] in the following manner. The L/D-

Table 1. NMR Spectroscopic Data for Mirabamide A (**1**) (CD_3CN–H_2O 5:1)

	δ_C[a]	δ_H[b] (*J* in Hz)	HMBC[c]	ROESY[d]
		ClHpr		
1	171.1			
2	50.1	4.99 br d (7.6)	1, 3, 4, 6, $1_{\beta\text{-OMeTyr}}$	3a
3a	33.3	2.48 br d (15.7)	4	2, 5
3b		2.23 dd (15.7, 7.6)	2	4
4	56.4	4.52 br s		3b, 5
5	33.1	1.91 m		6a, 4, 6b
6a	39.0	4.06 m	5, $1_{\beta\text{-OMeTyr}}$	5, $2_{\beta\text{-OMeTyr}}$
6b		3.51 m	5, $1_{\beta\text{-OMeTyr}}$	3
		β-OMeTyr		
1	172.3			
2	52.1	5.31 t (9.7)	1, 3, 1′, $1_{N\text{MeThr}}$	3, 2′, NH, $6a_{\text{ClHpr}}$
3	84.6	4.29 d (9.7)	2, 1′, 2′, OMe-3	2, 2′, NH, OMe-3,
1′	131.8			
2′, 6′	130.8	7.32 dd (8.2, 1.2)	1′, 3′, 4′	2, 3, OMe-3, $4_{N\text{MeThr}}$
3′, 5′	117.4	7.01 dd (8.2, 1.2)	1′, 2′, 4′	1_{Rha}, $4_{N\text{MeThr}}$
4′	157.3			
OMe-3	57.3	3.03 s	3	3
NH		7.75 d (9.7)	2, $1_{N\text{MeThr}}$	2, 2′, $2_{N\text{MeTh}}$
		*N*MeThr		
1	169.0			
2	64.1	4.32 d (9.9)	1, 3, 4, NMe, 1_{Ala}	4, *N*Me
3	63.8	3.85 m	2	4, *N*Me
4	19.7	0.36 d (5.9)	3	2, 3, $NH_{\beta\text{-OMeTyr}}$
NMe	31.1	3.04 s	2, 1_{Ala}	2, 3, 2_{Ala}
		Ala		
1	174.6			
2	48.5	4.45 m	1, 3, 1_{Gly1}	3, NH, $NMe_{N\text{MeThr}}$
3	15.6	1.41 d (7.2)	1, 2	2, NH
NH		6.98 d (5.9)	2, 3, 1_{Gly1}	2, 3, NH_{Gly1}
		Gly1		
1	171.8			
2a	42.7	4.12 dd (17.5, 8.3)	1	2b, NH
2b		3.53 dd (17.5, 8.3)	1	2a
NH		8.30 br t (5.30)	$1_{\text{3-OMeAla}}$	2a, $2_{\text{3-OmeAla}}$
		3-OMeAla		
1	171.9			
2	56.8	4.22 m	1, 3, $1_{\text{3-OHLeu}}$	3a, 3b. OMe-3, NH, NH_{Gly1}
3a	71.1	3.80 m	1, 2, OMe-3	2
3b		3.70 m	1, 2, OMe-3	2
OMe-3	59.5	3.31 s	3	2
NH		8.00 d (4.8)	2, 3, $1_{\text{3-OHLeu}}$	3a, 3b, $2_{\text{3-OHLeu}}$
		3-OHLeu		
1	172.7			
2	55.6	5.14 d (10.7)	1, 3, 4, $1_{\text{3,4-DiMeGln}}$	5, 6, NH
3	80.9	5.17 d (11.6)	4, 5, 1_{ClHpr}	5, 6, NH
4	29.0	1.91 m	3, 5, 6	5, 6
5	20.4	0.95 d (6.3)	3, 4, 6	3, 4
6	18.5	0.78 d (6.3)	3, 4, 5	3, 4
NH		8.68 d (10.7)	1, $1_{\text{3,4-DiMeGln}}$	4, $2_{\text{3,4-DiMeGln}}$
		3,4-DiMeGln		
1	175.2			
2	58.7	4.24 dd (9.2, 3.9)	1, 3, 4, 1_{Dab}	3, 4, Me-3, Me-4
3	37.4	2.12 m		2, 4, Me-3
4	42.1	2.59 m	3	2, 3, Me-3, Me-4, NH_2-5
5	180.2			
Me-3	14.1	1.00 d (6.8)	2, 3, 4	2, 3, 4
Me-4	15.2	1.14 d (6.3)	3, 4, 5	3, 4, NH_2-5
NH		9.18 d (3.9)		
NH_2-5		7.09 br s	5	4, Me-4
		6.60 br s	5	
		Dab		
1	171.1			
2	55.2	4.57 t (7.0)	1, 3, 4, 1_{Thr}	3, 4, NH
3	49.4	3.82 m	2, 4	4
4	15.3	1.24 d (6.3)	2, 3	3
NH		8.44 (7.8)	1_{Thr}	2, 2_{Thr}
NH_2-3		Na		
		Thr		
1	173.0			
2	59.5	4.43 m	1, 3, 4, 1_{Gly2}	3, 4, NH

Table 1. Continued

	δ_C[a]	δ_H[b] (*J* in Hz)	HMBC[c]	ROESY[d]
3	68.2	4.22 m		2
4	19.6	1.11 d (6.2)	2, 3	2, 3, NH
NH		7.71 (9.0)	2, 3, 1_{Gly2}	4, $2a_{Gly2}$, $2b_{Gly2}$
		Gly2		
1	172.3			
2a	43.7	4.04 dd (16.6, 6.2)	1, 1_{Dhtda}	NH_{Thr}
2b		3.80 dd (16.6, 6.2)	1, 1_{Dhtda}	NH_{Thr}
NH		8.20 t (6.2)	2, 1_{Dhtda}	
		Dhtda		
1	178.5			
2	78.8			
3	72.7	4.78 d (10.3)	4, 5	7, Me-2, Me-6
4	125.5	5.42 dd (12.3, 10.3)	2, 3, 6	3, Me-2
5	138.8	6.11 dd (12.3, 4.1)	3, 6, 7, Me-6	7, Me-6
6	131.9			
7	139.6	5.20 d (9.9)	5, 8, 9, Me-6, Me-8	3, 5, 9a, Me-8
8	35.0	2.32 m		7, 9b, 10
9a	30.9	1.21 m	7, 8, 10, Me-8	7
9b		1.34 m	7, 8, 10, Me-8	8
10	12.4	0.82 t (7.3)	8, 9	8, 9
Me-2	22.4	1.17 s	1, 2, 3	3, 4, 7
Me-6	16.8	1.74 d (3.8)	5, 6, 7	3, 5, 8, Me-2, Me-6, Me-8
Me-8	21.0	0.90 d (6.5)	7, 8, 9	7, 8, 9a, 9b
		Rha		
1	98.8	5.40 br s	2, 3, 5, $4'_{\beta\text{-OMeTyr}}$	2, $3'_{\beta\text{-OMeTyr}}$
2	71.2	3.97 br d (3.5)	3, 4	3
3	71.7	3.78 dd (9.0, 2.5)	4	5
4	73.1	3.39 t (9.0)	3, 5, 6	6
5	70.2	3.56 m	1, 3, 6	6
6	17.9	1.14 d (6.1)	4, 5	4

[a] Recorded at 600 MHz; referenced to residual CD_3CN at δ 1.93 ppm. [b] Recorded at 150 MHz; referenced to residual CD_3CN at δ 117.7 ppm. [c] Proton showing HMBC correlation to indicated carbon. [d] Proton showing ROESY correlation to indicated proton.

FDLA derivatives of ClHpr were detected at retention times of 29.5 and 15.7 min, while the L-FDLA derivative was detected at 29.5 min on the reconstructed ion chromatogram for *m/z* 456 $[M-H]^-$ (see Experimental Section). As in the case of homoproline, the D-FDLA derivative of ClHpr elutes prior to that of the L-LFDLA.[10] In addition, the small $J_{H,H}$ value displayed by $H\text{-}4_{ClHpr}$ (δ 4.52, br s) along with strong ROEs between axial $H\text{-}2_{ClHpr}$ (4.99, br d, J = 7.6 Hz) and equatorial $H\text{-}3a_{ClHpr}$ (2.48, d, J = 15.7 Hz) and between $H\text{-}4_{ClHpr}$ and equatorial $H\text{-}3b_{ClHpr}$ (2.23, dd, J = 15.7, 7.6 Hz) established the absolute configuration of $C\text{-}4_{ClHpr}$ as *S*.

Due to decomposition of the β-OMeTyr residue during acid hydrolysis of **1**, we were unable to use Marfey's methods to establish the absolute configuration for this residue. Zampella et al. avoided this problem in the structure elucidation of callipeltin A by transforming β-OMeTyr to β-OMe Asp via ozonolysis prior to acid hydrolysis and derivatization.[12] In the case of mirabamide A, where the β-OMeTyr residue is glycosidated, oxidation under the reported conditions was unsuccessful, and limited material prevented us from exploring other approaches. Although we were unable to unambiguously determine the absolute configuration of the β-OMeTyr unit through analysis of degradation or derivatization techniques, analysis of our NMR data and comparison with published data for β-OMeTyr provide strong support for assigning the absolute configuration of this residue as follows. The combination of a large $^3J_{H\text{-}H}$ coupling constant of 9.7 Hz between $H\text{-}2_{\beta\text{-OMeTyr}}$ and $H\text{-}3_{\beta\text{-OMeTyr}}$ and a strong ROE correlation between the $NH_{\beta\text{-OMeTyr}}$ proton at δ 7.75 and the $H\text{-}2'_{\beta\text{-OMeTyr}}$ aromatic proton at δ 7.32 establishes the relative configuration of the β-OMeTyr residue as *erythro*.[13] By using synthetic standards of all four β-OMeTyr stereoisomers, Oku et al. showed the absolute configuration of the β-OMeTyr residue in papuamide B to be *R*-β-OMe-D-Tyr, while neamphamide A contains the C-2 epimer *R*-β-OMe-L-Tyr.[14] In that study, they reported the β-oxymethine proton (H-2) of *R*-β-OMe-D-Tyr as a doublet ($^3J_{H\text{-}H}$ = 9.3 Hz) at δ 4.24, and the equivalent proton in *R*-β-OMe-L-Tyr as a broadened singlet at δ 5.03.[14] Similar to values reported for *R*-β-OMe-D-Tyr in papuamide B[4] the ^{1}H NMR spectrum of mirabamide A contains a doublet ($^3J_{H\text{-}H}$ = 9.7 Hz) at δ 4.29 that corresponds to the β proton (H-2) of β-OMeTyr. On the basis of these data and the structural similarities between papuamide B and compound **1**, it is likely that the absolute configuration of the β-OMeTyr unit in mirabamides A–D is *R*-β-OMe-D-Tyr. Last, the sugar unit was determined to be L-rhamnose by direct comparison of GC retention times between the trimethylsilylated hydrolysate (2 N HCl) of **1** and the trimethylsilyl derivative of an authentic sample of L-rhamnose using a chiral capillary column.

The HRESIMS of compound **2** displayed an isotopic pattern of the major ion peak $[M+H]^+$, 3:1, at *m/z* 1579.7531 and 1581.7642, suggesting a molecular formula of $C_{72}H_{111}ClN_{12}O_{25}$ (calcd for $C_{72}H_{112}ClN_{12}O_{25}$, 1579.7550). Its ^{1}H NMR spectrum in comparison to that of **1** showed just a few differences including the presence of an additional olefinic signal at δ 6.71 (1H, q, J = 7.2 Hz) and the absence of the signal at δ 3.82 (1H, m) ascribable to the β-methine group of the Dab residue in **1**. Furthermore, HMBC correlations from the olefinic proton at δ 6.71 ($H\text{-}3_{Aba}$) to the carbonyl resonance at δ 166.5 ($C\text{-}1_{Aba}$) and from the methyl protons at δ 1.67 ($Me\text{-}4_{Aba}$) to the olefinic carbon resonances at δ 134.5 ($C\text{-}3_{Aba}$) and 129.6 ($C\text{-}2_{Aba}$) indicated the presence of 2,3-dehydro-2-aminobutanoic acid (Aba). Finally, a detailed analysis of the 2D NMR data (2D-HOHAHA, COSY, HSQC, HMBC, ROESY) of **2** indicated that it differed from **1** only by the presence of the Aba instead of the Dab residue. Analysis of the derivatized hydrolysate (5 N) of **2** by LC-MS according to the advanced Marfey's method indicated the same absolute configuration for each amino acid residue as in **1**. Chiral GC analysis of the trimethylsilylated hydrolysate (1 N) of **2** also indicated an L configuration for the α-rhamnose unit. Finally ROESY correlations between the Aba NH (δ 9.0, br s) and Aba methyl group (δ 1.67, d, J = 7.2 Hz) indicated a *Z* geometry for the double bond.

The HRESIMS of **3** displayed an isotopic pattern of the major ion peak $[M + H]^+$, 3:1, at *m/z* 1450.7239 and 1452.7295 ($C_{66}H_{104}ClN_{13}O_{21}$, calcd for $C_{66}H_{105}ClN_{13}O_{21}$, 1450.7237), and compound **4** was assigned the molecular formula $C_{72}H_{115}N_{13}O_{25}$ (*m/z* 1562.8177 $[M + H]^+$, calcd for $C_{72}H_{116}N_{13}O_{25}$, 1562.8205), indicating **3** and **4** were 146 and 34 mu lower than **1**, respectively. A careful analysis of the NMR data (^1H, ^{13}C, HSQC, HMBC, DQF-COSY, 2D-HOHAHA, ROESY) established that **3** and **4** were the desrhamnsose and deschloro analogues of **1**, respectively. Once again, LC-MS analysis of the L/D-FDLA-derivatized hydrolysates of **3** and **4** revealed that all the amino acid residues possessed identical configurations to those in **1**. In a similar fashion, the absolute configuration of the homoproline residue in **4** was established as L.

Callipeltin A, isolated from a New Caledonia sponge *Callipelta* sp.,[15] papuamides A–D, obtained from sponges *T. mirabilis* and *T. swinhoei* from Papua New Guinea,[4] and neamphamide A, isolated from the Papua New Guinea sponge *Neamphius huxlei*,[16] belong to a family of cyclic depsipeptides, all of which have been reported to have potent HIV inhibitory activities. This family of peptides is characterized by the common occurrence of the unusual amino acid residues 3,4-dimethylglutamine and β-methoxytyrosine, and N-terminal aliphatic hydroxy acid moieties. This combination of unique structural features and biological activities has generated interest among many synthesis groups.[17]

The potential role of the β-methoxytyrosine residue in the HIV inhibitory activity of this family of peptides has been suggested recently.[18] Theopapuamide, a new depsipeptide isolated from *T. swinhoei* collected in Papua New Guinea, shows a skeleton similar to callipeltin and neamphamide A, differing mainly in the lack of the β-methoxytyrosine residue. However, theopapuamide did not show any appreciable HIV inhibitory activity, suggesting that the activity of this family of compounds is due to the β-methoxytyrosine residue and not to the 3,4-dimethylglutamine, as previously postulated by Acevedo et al.[17c] The structural features of mirabamides make them perfect candidates to evaluate the influence of the β-methoxytyrosine residue on the HIV inhibitory activity of this compound class.

To determine the effects of the mirabamides on HIV-1 infection, each was tested against two different viral strains (HXB2, a CXCR4-using or T-cell-tropic virus, and SF162, a CCR5-using or macrophage-tropic virus) in HIV-1 neutralization assays employing pseudotyped viruses. In addition, because mechanistic studies for this class of peptides are thus far lacking, mirabamides A–D (**1**–**4**) were tested in an HIV-1 envelope-mediated cell fusion assay to determine whether they act at the early steps of infection, namely viral entry. As seen in Figure 1a and Table 2, mirabamides A, C, and D potently inhibit HXB2 infection of TZM-bl host cells with IC_{50} values of 140 nM for mirabamides A and C and 190 nM for mirabamide D. In contrast, mirabamide B was significantly less active, failing to inhibit HXB2 at concentrations as high as 50 μM. Relative to HXB2, compounds **1**, **3**, and **4** showed slightly reduced potency toward SF162 (Figure 1b), with IC_{50} values of 400 nM for mirabamide A and around 1 μM for mirabamides C and D. As with HXB2, mirabamide B only weakly inhibited SF162.

Results for testing mirabamides A–D and a standard of papuamide A in a fusion assay are shown in Figure 1c. Apparent from the plots, **1**, **3**, and **4** as well as papuamide A each inhibit HIV-1 envelope-mediated fusion with activities comparable to those observed in the neutralization assays. Mirabamide A and papuamide A (**5**) were found to be the most potent inhibitors in the fusion assay, with respective IC_{50} values of 41 and 73 nM, while mirabamides C and D inhibit fusion at low micromolar concentrations. Thus, similar to papuamides A and B, callipeltin A, and neamphamide A, mirabamides also exhibit potent anti-HIV activity toward multiple strains of HIV. Further, our results demonstrate that this class of peptides inhibits HIV-1 at the level of membrane fusion, presumably through interactions with HIV-1 envelope glycoproteins.

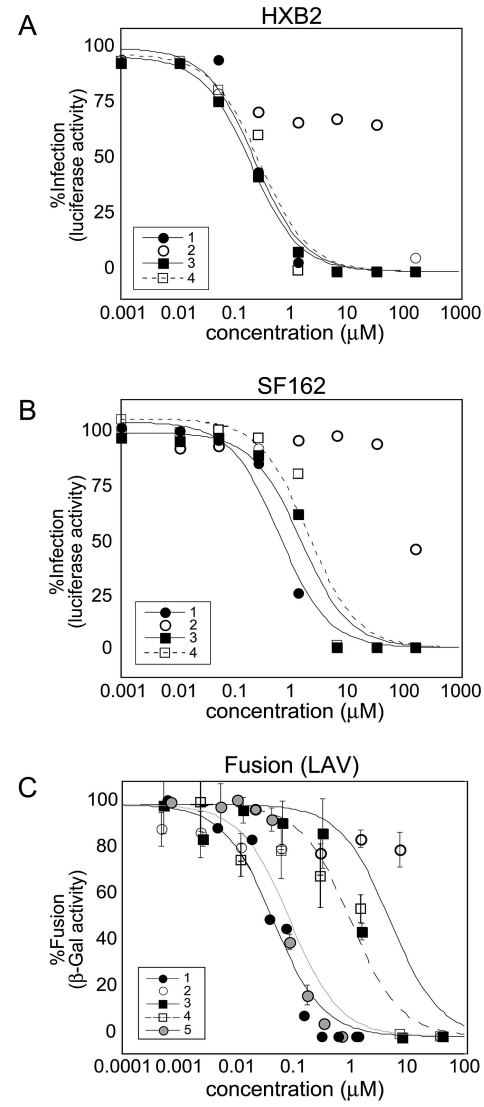

Figure 1. Inhibition of HIV-1 in neutralization and fusion assays. Plots showing effects of mirabamides A–D on neutralization of viral particles from strains (a) HXB2 (T-cell-tropic) and (b) SF162 (macrophage-tropic). TZM-bl indicator cells (expressing CXCR4, CCR5, and CD4) were used for neutralization assays; standard deviations averaged 15% in all experiments. (c) Inhibition curves showing effect of mirabamides A–D and papuamide A on HIV-1 envelope-mediated cell fusion against LAV (T-cell-tropic). Compounds are indicated in legends for each plot.

Table 2. IC_{50} Values (μM) for HIV-1 Inhibition Assays

compound	HXB2[a]	SF162[b]	LAV[c]
1	0.140 ± 0.04	0.40 ± 0.08	0.041 ± 0.01
2	>50	>50	>10
3	0.144 ± 0.01	1.01 ± 0.33	1.3 ± 0.5
4	0.189 ± 0.05	1.31 ± 0.40	3.9 ± 0.9
5	Nt	nt	0.073 ± 0.02

[a] Neutralization assay using viral particles pseudotyped with envelopes from HXB2. [b] Neutralization assay using viral particles pseudotyped with envelopes from SF162. [c] HIV-1 envelope-mediated cell fusion assay using LAV; nt (not tested).

Mirabamide B was consistently found to be less potent than mirabamides A, C, and D in both neutralization and fusion assays. Mirabamide B is the only peptide of the four to contain a 2,3-dehydro-2-aminobutanoic acid residue in place of the 2,3-diaminobutanoic acid residue found in **1**, **3**, and **4**, as well as papuamides

Table 3. IC_{50} Values (μM) for Cytotoxicity Assays

compound	HCT-116[a]	TZM-bl[b]
1	2.22 ± 0.4	1.8 ± 0.8
2	nt	nt
3	nt	2.2 ± 0.1
4	nt	3.9 ± 1.3
5	3.5 ± 1.7	nt

[a] Human colon tumor cell line. [b] Host cell line for neutralization assay; nt (not tested).

A and B. Thus, the Dab residue in this class of peptides appears to be important for anti-HIV activity. As for the role of the β-OMe Tyr residue, we were somewhat surprised to find that mirabamide A, which contains the rhamnosylated β-OMe Tyr residue, was observed to be the most or among the most potent of the four peptides described here. This result is not in conflict with the notion that the β-OMe Tyr residue is critical for anti-HIV activity, as suggested by Ratnayake et al.[18] Rather, it indicates that β-OMe Tyr residues bearing substitution at the 4′ position can be tolerated with no deleterious effect on antiviral activity and that the presence of a free 4′ hydroxyl on the Tyr unit is not essential. One hypothesis that would be consistent with all of the results reported to date–namely, that peptide **1** is equipotent to papuamide A (which also contains a β-OMe Tyr residue) while theopapauamide (which lacks a β-OMe Tyr residue) is inactive–is that this residue imparts a specific conformation required for binding to target protein/s involved in HIV-1 entry.

Mirabamides A, C, and D were tested for cytotoxicity toward the tumor cell line HCT-116 and each of the cell lines used in the anti-HIV assays (Table 3). Mirabamide A and papuamide A inhibited the growth of HCT-116 cells with IC_{50} values of 2.2 and 3.0 μM, respectively. None of the peptides were found to be toxic to B-SC-1 cells under the same conditions used in the fusion assays (3 h treatment). However, compounds **1**, **3**, and **4** were each found to be cytotoxic to TZM-bl cells under conditions used in the neutralization assay (incubation for 24 h) with IC_{50} values around 2–4 μM. Thus, in our hands the therapeutic window for these peptides, which ranges from 3 to 13 depending on the assay and cell line used, is appreciably lower than previous reports. Antimicrobial and antifungal assays revealed that mirabamides C and D strongly inhibited growth of *B. subtilus* at loadings of 1 μg/disk, displaying a zone of growth inhibition of 9 mm, while mirabamides A and B were slightly less potent, displaying similarly sized zones of inhibition at 5 μg/disk. Mirabamides A–C showed antifungal activity against *C. albicans*, displaying a zone of growth inhibition of 9 mm at 5 μg/disk. None of the peptides inhibited the growth of *Escherichia coli*, *Pseudomonas aeruginosa*, or *Staphylococcus aureus* at loads as high as 25 μg/disk.

In summary, we have discovered four new depsipeptides, mirabamides A–D, that add to a small class first exemplified by the papuamides. Mirabamides A, C, and D potently inhibit HIV-1 in both neutralization and fusion assays, providing evidence that this class of peptides can act at the early steps of HIV-1 infection. Mirabamides A–C contain two previously undescribed amino acids, 4-chlorohomoproline and β-methoxytyrosine 4′-*O*-α-L-rhamnopyranoside, neither of which effect their anti-HIV activities, thereby demonstrating that the β-OMe Tyr residue alone is not essential for anti-HIV activity as previously suggested. The potency of this class of peptides toward HIV-1 warrants the many ongoing synthetic studies.

Experimental Section

General Experimental Procedures. Optical rotations were measured with a Perkin-Elmer 341 polarimeter, and UV spectra were recorded on an Agilent 8453 spectrophotometer. NMR spectra were recorded in CD_3OD, $CDCl_3$, d_6-DMSO, or 5:1 CD_3CN–H_2O on a Bruker DRX-600 spectrometer (^1H at 600 MHz, ^{13}C at 150 MHz). DQF-COSY, 2D-HOHAHA, HSQC, HMBC, and ROESY (τ_m = 400 ms) experiments were recorded using standard pulse programs, all of which included water suppression (Watergate). HSQC experiments were optimized for $^1J_{C\text{-}H}$ = 145 Hz, and HMBC spectra were optimized for $^{2,3}J_{C\text{-}H}$ = 5 Hz. The accurate mass electrospray ionization (ESI) mass spectra were measured on a Waters LCT Premier time-of-flight (TOF) mass spectrometer. The instrument was operated in Ω-mode at a nominal resolution of 10 000. The electrospray capillary voltage was set at 2 kV and the sample cone voltage at 60 V. The desolvation temperature was set to 275 °C, and nitrogen was used as the desolvation gas with a flow rate of 300 L/h. Accurate masses were obtained using the internal reference standard method. The sample was introduced into the mass spectrometer via the direct loop injection method. Both positive and negative ion accurate mass data were achieved simply by reversing the instrument's operating polarity. LC-MS analyses were carried out using an Agilent 1100 MSD integrated LC-MS system employing negative ion ESI mode.

Sponge Material. The sponge was collected from an open reef off Nama Island, southeast of Chuuk Lagoon, in the Federated States of Micronesia, at a depth of 50 m, on August 25, 1994. The sponge was thickly encrusting with rounded conical projections and apical oscules and was slightly compressible. The surface was slightly fuzzy to the touch, the color in life is reddish-brown, and the interior is orange. The sponge is most closely comparable with *Siliquariaspongia mirabilis* (de Laubenfels, 1954) (Lithistid Demospongiae: family Theonellidae), but lacks the characteristic nonarticulated tetracladine desmas that characterize the genus.[19] A voucher specimen has been deposited at the Natural History Museum, London, United Kingdom (BMNH 2007.7.9.1).

Extraction and Isolation. Samples were frozen immediately after collection and shipped on dry ice to Frederick, MD, where they were freeze-dried and extracted with H_2O (OCDN 2547). A 6 g portion of the extract was partitioned with *n*-BuOH–H_2O (1:1) to afford a dried *n*-BuOH extract (0.7 g), which was fractionated on a Sephadex LH-20 column (50 × 2.5 cm) using MeOH as mobile phase. Fractions containing peptides were combined, and the solvent was removed in vacuo to give 148 mg of a yellow film, which was subsequently purified by reversed-phase HPLC (Synergi Fusion C18, 250 × 10 mm, 4 μm, DAD at 220 and 280 nm) eluting with a linear gradient of 50–80% MeOH in 0.05% TFA in 50 min to afford compounds **1** (4.6 mg, t_R = 29.4 min), **2** (0.8 mg, t_R = 47.4 min), **3** (1.2 mg, t_R = 30.8 min), and **4** (0.3 mg, t_R = 30.9 min).

Mirabamide A (1): colorless, amorphous powder; $[\alpha]^{20}_D$ −1.2 (*c* 0.17, MeOH); UV (MeOH) λ_{max} (log ε) 203 (4.65), 223 (sh) (4.38), 272 (3.4) nm; ^1H and ^{13}C NMR data, see Table 1; HRESIMS *m/z* 1596.7753 $[M + H]^+$ (calcd for $C_{72}H_{115}ClN_{13}O_{25}$, 1596.7816).

Mirabamide B (2): colorless, amorphous powder; $[\alpha]^{20}_D$ −2.0 (*c* 0.10, MeOH); UV (MeOH) λ_{max} (log ε) 206 (4.63), 221 (sh) (4.29), 276 (3.3) nm; ^1H and ^{13}C NMR data for ClHpr, β-OMeTyr, *N*MeThr, Ala, Gly1, 3-OMeAla, 3-OHLeu, Thr, Gly2, Dhtda, and Rha are identical to those reported for **1** in Table 1; ^1H NMR (CD_3CN–H_2O, 5:1, 600 MHz) Aba: δ 6.71 (1H, q, J = 7.2 Hz, H-3), 1.67 (3H, d, J = 7.2 Hz, Me-4), 9.00 (br s, NH), 3,4-DiMeGln: 4.29 (1H, dd, J = 9.2, 3.9 Hz, H-2), 2.12 (1H, m, H-3), 2.54 (1H, m, H-4), 0.97 (3H, d, J = 6.8 Hz, Me-3), 1.14 (3H, d, J = 6.3 Hz, Me-4), 8.14 (1H, d, J = 3.9 Hz, NH), 7.09 (1H, br s, NH_2-5a), 6.60 (1H, br s, NH_2-5b); ^{13}C NMR (CD_3CN–H_2O, 5:1, 150 MHz) Aba: 166.5 (C-1), 129.6 (C-2), 134.5 (C-3), 13.7 (Me-4), 3,4-DiMeGln: 175.2 (C-1), 58.8 (C-2), 37.4 (C-3), 41.2 (C-4), 180.2 (C-5), 13.3 (Me-3), 15.2 (Me-4); HRESIMS *m/z* 1579.7531 $[M + H]^+$ (calcd for $C_{72}H_{112}ClN_{12}O_{25}$, 1579.7550).

Mirabamide C (3): colorless, amorphous powder; $[\alpha]^{20}_D$ −1.5 (*c* 0.06, MeOH); UV (MeOH) λ_{max} (log ε) 206 (4.64), 222 (sh) (4.29), 273 (3.3) nm; ^1H and ^{13}C NMR data for ClHpr, *N*MeThr, Ala, Gly1, 3-OMeAla, 3-OHLeu, 3,4-DiMeGln, Dab, Thr, Gly2, and Dhtda are identical to those reported for **1** in Table 1; ^1H NMR (CD_3CN–H_2O, 5:1, 600 MHz) β-OMeTyr: δ 5.28 (1H, t, J = 9.7, H-2), 4.22 (1H, d, J = 9.7, H-3), 7.18 (2H, dd, J = 8.2, 1.2, H-2′/H-6′), 6.74 (2H, dd, J = 8.2, 1.2, H-3′/H-5′), 3.03 (3H, s, OMe-3), 7.75 (1H, d, J = 9.7, NH); ^{13}C NMR (CD_3CN–H_2O, 5:1, 150 MHz) β-OMeTyr: 172.3 (C-1), 52.1 (C-2), 84.7 (C-3), 128.9 (C-1′), 130.7 (C-2′/C-6′), 116.1 (C-3′/C-5′), 158.3 (C-4′), 57.3 (OMe-3); HRESIMS *m/z* 1450.7239 $[M + H]^+$ (calcd for $C_{66}H_{105}ClN_{13}O_{21}$, 1450.7237).

Mirabamide D (4): colorless, amorphous powder; $[\alpha]^{20}_D$ −2.5 (*c* 0.04, MeOH); UV (MeOH) λ_{max} (log ε) 204 (4.61), 222 (sh) (4.28), 271 (3.3) nm; ^1H and ^{13}C NMR data for β-OMeTyr, *N*MeThr, Ala, Gly1, 3-OMeAla, 3-OHLeu, 3,4-DiMeGln, Dab, Thr, Gly2, Dhtda, and

Rha are identical to those reported for **1** in Table 1; ^{1}H NMR (CD_3CN–H_2O, 5:1, 600 MHz) Hpr: δ 4.99 (1H, d, J = 7.6, H-2), 2.09 (1H, m, H-3a), 1.67 (1H, m, H-3b), 1.64 (1H, m, H-4a), 1.14 (1H, m, H-4b), 1.68 (1H, m, H-5a), 1.36 (1H, m, H-5b), 4.03 (1H, m, H-6a), 3.08 (1H, m, H-6b); ^{13}C NMR (CD_3CN-H_2O 5:1, 150 MHz) Hpr: 170.8 (C-1), 53.8 (C-2), 26.5 (C-3), 21.0 (C-4), 25.3 (C-5), 44.4 (C-6); HRESIMS *m/z* 1562.8177 $[M + H]^+$ (calcd for $C_{72}H_{116}N_{13}O_{25}$, 1562.8205).

LC/MS Analysis of L/D-FDLA Derivatives.[11] Approximately 0.2 mg of compounds **1**–**4** was separately hydrolyzed with 5 N HCl (LabChem Inc., traceable to NIST) (0.8 mL) in an Ace high-pressure tube for 16 h at 90 °C. The hydrolysates were evaporated to dryness and dissolved in H_2O (100 μL). To a 50 μL aliquot of each were added 1 N $NaHCO_3$ (20 μL) and 1% 1-fluoro-2,4-dinitrophenyl-5-L-leucinamide (L-FDLA or D-FDLA solution in acetone, 100 μL), and the mixtures were heated to 40 °C for 40 min The solutions were cooled to room temperature, neutralized with 2 N HCl (20 μL), and evaporated to dryness. The residues were dissolved in CH_3CN and analyzed by LC-MS. The analysis of the L- and L/D-FDLA (mixture of D- and L-FDLA) derivatives was performed on a Phenomenex Jupiter Proteo C12 column (4 μm, 150 × 4.6 mm). Aqueous CH_3CN containing 0.01 M TFA was used as a mobile phase eluting with a linear gradient of 25–70% CH_3CN in 45 min at a flow rate of 0.5 mL/min. An Agilent Series 1100 MSD mass spectrometer was used for detection in ESI (negative) mode. The fragmentor and capillary voltage were kept at 70 and 1000 V, respectively, and the ion source was kept at 350 °C. A mass range of *m/z* 100–1000 was scanned in 0.1 min. Retention times (t_R, min) of the FDLA-derivatized amino acids: (2*R*,3*R*)-3-hydroxyleucine 23.7, (2*S*,3*R*)-3-hydroxyleucine 30.5, *m/z* 440 $[M - H]^-$; L-3-OMeAla 23.9, D-3-OMeAla 27.1, *m/z* 412 $[M - H]^-$; L-*N*MeThr 19.7, D-*N*MeThr 21.0, *m/z* 426 $[M - H]^-$; L-Ala 24.4, D-Ala 27.0, *m/z* 382 $[M - H]^-$; L-Thr 19.5, D-Thr 23.1, *m/z* 412 $[M - H]^-$; L-Hpr 29.6, D-Hpr 28.4, *m/z* 422 $[M - H]^-$; L-ClHpr 28.9, D-ClHpr 28.1, *m/z* 456 $[M - H]^-$; (3*S*,4*R*)-dimethyl-L-glutamine 23.3, (3*S*,4*R*)-dimethyl-D-glutamine 24.3, *m/z* 467 $[M - H]^-$; (2*S*,3*R*)-diaminobutanoic acid 38.4, (2*R*,3*S*)-diaminobutanoic acid 41.3, *m/z* 467 $[M - H]^-$ (bis derivative).

Absolute Configuration of Rhamnose. A solution (0.2 mg each) of **1**, **2**, and **4** in 1 N HCl (0.25 mL) was stirred at 80 °C for 4 h. After cooling, the solution was concentrated by blowing with N_2. The residue was dissolved in 1-(trimethylsilyl)imidazole (40 μL) and pyridine (160 μL), and the solution was stirred at 60 °C for 15 min After drying the solution with a stream of N_2, the residue was separated by H_2O and CH_2Cl_2 (1 mL, 1:1 v/v). The CH_2Cl_2 layer was analyzed by GC using a Supelco β-Dextrin column (0.22 mm × 25 m). Temperatures of the injector and detector were 200 and 250 °C, respectively. A temperature gradient system was used for the oven starting at 50 °C and increasing up to 180 °C at a rate of 5 °C/min. Peaks corrresponding to the trimethylsilyl derivatives of L-rhamnose in the hydrolysates of **1**, **2**, and **4** eluted at 19.0 min, as did the trimethylsilyl derivative of an authentic sample of L-rhamnose. Peaks corresponding to L-rhamnose in the hydrolysates of **1**, **2**, and **4** coeluted with the L-rhamnose standard.

Biological Assays. HIV-1 Env-mediated cell fusion assays were performed as previously described.[20] All reagents were obtained from the NIH AIDS Research and Reference Reagent Program and include soluble CD4 (#7356) donated by Pharmacia, and recombinant vaccinia viruses expressing genes for LAV-derived HIV-1 envelope (vCB41, #3375), T7 polymerase (vP11T7gene1, #3356), β-galactosidase (vCB21R-LacZ, #3365), and CXCR4 (vCBYF1-fusin, #3364), all of which were donated by C. Broder, P. Kennedy, and E. Berger. B-SC-1 cells were used as both target and effector cells in all fusion assays. Effector cells were co-infected with vaccinia viruses encoding HIV-1 Env and β-Gal, and target cells were co-infected with CXCR4 and T7 polymerase-encoding viruses, each at an MOI of 2. Following a 2.5 h incubation in the presence of inhibitor at 37 °C, percent fusion was measured as a function of β-Gal activity on the substrate chlorophenol-red-β-D-galactopyranoside (A_{570}, Molecular Devices 96-well absorbance plate reader). Neutralization assays were conducted using viral particles pseudotyped with HIV-1 envelopes together with TZM-bl indicator cells (#8129, donated by J. C. Kappes and X. Wu), as described recently by Mascola and Montifiori.[21] Briefly, after overnight incubation at 37 °C in 96-well plates, pseudotyped viruses in the presence of varying concentrations of inhibitor (dissolved in H_2O or 20% EtOH in H_2O) were added to TZM-bl indicator cells. Following a 48 h incubation at 37 °C, the assays were developed using luciferase reagent and luminescence was read in relative light units (RLUs) on a luminescence counter (Perkin-Elmer 1450 MicroBeta). All HIV assays were performed in duplicate or triplicate on at least two different days. Standard errors in the neutralization assays average 15%.

Cytotoxicity assays were carried out using an MTT cell proliferation assay kit (American Type Culture Collection) according to instructions provided. Briefly, HCT-116, B-SC-1, or TZM-bl cells were seeded in 96-well tissue culture plates at a density of 2×10^4 cells/well in 50 μL of growth media and allowed to adhere for 18 h. Attached cells were incubated with inhibitors for either 3 h (to duplicate conditions used in the fusion assays) or 24 h (as controls for the neutralization assay), after which the media was either replaced or diluted 3-fold with fresh growth media. Following an additional 72 h incubation, cell viability was assessed upon treatment with MTT (A_{570}, Molecular Devices 96-well absorbance plate reader).

Antimicrobial Activity. Compounds **1**–**4** were tested for antimicrobial activity against *Pseudomonas aeruginosa* (ATCC 15442), *Escherichia coli* (ATCC 8739), *Staphylococcus aureus* (ATCC 25923), *Bacillus subtilis* (ATCC 49343), and *Candida albicans* (ATCC 90027) using a modified disk diffusion assay. Agar plates seeded with suspensions of bacteria or fungi were prepared by adding 500 μL of a 24 h culture of bacteria to 100 mL of autoclaved Antibiotic Medium 2 (AB2) containing 1% agar and cooled to 55 °C, or of fungi to Sabouraud dextrose agar (SDA) at 55 °C. Seeded liquid agar (10 mL) was transferred immediately to square Petri dishes and allowed to cool for 1 h. Control drugs used for each microorganism included kanamycin (50 μg) for *P. aeruginosa* and *S. aureus*, ampicillin (50 μg) for *E. coli*, choloroamphenicol (10 μg) for *B. subtilis*, and amphotericin B (25 μg) for *C. albicans*. Following incubation at 37 °C for 18 h zones of inhibition resulting from antibiotics or depsipeptides (1–25 μg) were measured.

Acknowledgment. We thank the Coral Reef Research Foundation, D. Newman, and the state of Chuuk, Federated States of Micronesia, for facilitating sample acquisition; J. Lloyd and T. Spande for HRMS and GCMS data, respectively; NCI for an authentic sample of papuamide A; and L. Colin for helpful discussions. The AIDS Research and Reference Reagent Program, Division of AIDS, NIAID, NIH, is acknowledged for all reagents and cell lines used in the HIV-1 assays. This work was supported in part by the NIH Intramural Research Program (NIDDK) and the Intramural AIDS Targeted Antiviral Program, Office of the Director, NIH (C.A.B.).

Supporting Information Available: ^{1}H NMR, HSQC, HMBC, 2D-HOHAHA, DQF-COSY, and ROESY spectra for compounds **1** and **2**. This material is available free of charge via the Internet at http://pubs.acs.org.

References and Notes

(1) (a) Donia, M.; Hamman, M. T. *Lancet Infect. Dis.* **2003**, *3*, 338–348. (b) Gochfeld, D. J.; El Sayed, K. A.; Yousaf, M.; Hu, J. F.; Bartyzel, P.; Dunbar, D. C.; Wilkins, S. P.; Zjawiony, J. K.; Schinazi, R. F.; Wirtz, S. Schlueter; Tharnish, P. M.; Hamann, M. T. *Mini-Rev. Med. Chem.* **2003**, *3*, 401–424. (c) Newman, D. J.; Cragg, G. M. J. *Nat. Prod.* **2004**, *67*, 1216–1238. (d) Rawat, D. S.; Joshi, M. C.; Joshi, P.; Atheaya, H. *Anti-Cancer Agents Med. Chem.* **2006**, *6*, 33–40.

(2) Bewley, C. A.; Faulkner, D. J. *Angew. Chem., Int. Ed.* **1998**, *37*, 2162–2178.

(3) Hamada, T.; Matsunaga, S.; Yano, G.; Fusetani, N. *J. Am. Chem. Soc.* **2005**, *127*, 110–118.

(4) Ford, P. W.; Gustafson, K. R.; McKee, T. C.; Shigematsu, N.; Maurizi, L. K.; Pannell, L. K.; Williams, D. E.; Dillip de Silva, E.; Lassota, P.; Allen, T. M.; Van Soest, R.; Andersen, R. J.; Boyd, M. R. *J. Am. Chem. Soc.* **1999**, *121*, 5899–5909.

(5) Okada, Y.; Matsunaga, S.; van Soest, R. W. M.; Fusetani, N. *Org. Lett.* **2002**, *4*, 3039–3042.

(6) Bewley, C. A.; Faulkner, D. J. *J. Org. Chem.* **1994**, *59*, 4849–4852.

(7) Nakao, Y.; Fujita, M.; Warabi, K.; Matsunaga, S.; Fusetani, N. *J. Am. Chem. Soc.* **2000**, *122*, 10462–10463.

(8) Matsunaga, S.; Fusetani, N.; Kato, Y.; Hirota, H. *J. Am. Chem. Soc.* **1991**, *113*, 9690–9692.

(9) (a) Shin, H. J.; Matsuda, H.; Murakami, M.; Yamaguchi, K. *J. Org. Chem.* **1997**, *62*, 1810–1813. (b) Schmidt, E. W.; Bewley, C. A.; Faulkner, D. J. *J. Org. Chem.* **1998**, *63*, 1254–1258. (c) Neuhof, T.; Schmieder, P.; Preussel, K.; Dieckmann, R.; Pham, H.; Bartl, F.; von Dohren, H. *J. Nat. Prod.* **2005**, *68*, 695–700. (d) Neuhof, T.; Schmieder, P.; Seibold, M.; Preussel, K.; von Döhren, H. *Biorg. Med.*

Chem. Lett. **2006**, *16*, 4220–4222. (e) Pluotno, A.; Shmuel, C. *Tetrahedron* **2005**, *61*, 575–583.
(10) He, H.; Williamson, R. T.; Shen, B.; Graziani, E. I.; Yang, H. Y.; Sakya, S. M.; Petersen, P. J.; Carter, G. T. *J. Am. Chem. Soc.* **2002**, *124*, 9729–9736.
(11) (a) Fujii, K.; Ikai, Y.; Oka, H.; Suzuki, M.; Harada, K.-I. *Anal. Chem.* **1997**, *69*, 5146–5151. (b) Fujii, K.; Ikai, Y.; Mayumi, T.; Oka, H.; Suzuki, M.; Harada, K.-I. *Anal. Chem.* **1997**, *69*, 3346–3352.
(12) Zampella, A.; D'Orsi, R.; Sepe, V.; Casapullo, A.; Monti, M. C.; D'Auria, M. V. *Org. Lett.* **2005**, *7*, 3585–3588.
(13) Matsumori, N.; Kaneno, D.; Murata, M.; Nakamura, H.; Tachibana, K. *J. Org. Chem.* **1999**, *64*, 866–876.
(14) Oku, N.; Krishnamoorthy, R.; Benson, A. G.; Ferguson, R. L.; Lipton, M. A.; Phillips, L. R.; Gustafson, K. R.; McMahon, J. B. *J. Org. Chem.* **2005**, *70*, 6842–6847.
(15) Zampella, A.; D'Auria, M. V.; Paloma, L. G.; Casapullo, A.; Minale, L.; Debitus, C.; Henin, Y. *J. Am. Chem. Soc.* **1996**, *118*, 6202–6209.
(16) Oku, N.; Gustafson, K. R.; Cartner, L. K.; Wilson, J. A.; Shigematsu, N.; Hess, S.; Pannell, L. K.; Boyd, M. R.; McMahon, J. B. *J. Nat. Prod.* **2004**, *67*, 1407–1411.
(17) (a) Liang, B.; Carroll, P. J.; Joullie, M. M. *Org. Lett.* **2000**, *2*, 4157–4160. (b) Okamoto, N.; Hara, O.; Makino, K.; Hamada, Y. *Tetrahedron: Asymmetry* **2001**, *12*, 1353–1358. (c) Acevedo, C. M.; Kogut, E. F.; Lipton, M. A. *Tetrahedron* **2001**, *57*, 6353–6359. (d) Thoen, J. C.; Morales-Ramos, Á. I.; Lipton, M. A. *Org. Lett.* **2002**, *4*, 4455–4458. (e) Guerlavais, V.; Carroll, P. J.; Joullie, M. M. *Tetrahedron: Asymmetry* **2002**, *13*, 675–680. (f) Zampella, A.; Sorgente, M.; D'Auria, M. V. *Tetrahedron: Asymmetry* **2002**, *13*, 681–685. (g) Zampella, A.; D'Auria, M. V. *Tetrahedron: Asymmetry* **2002**, *13*, 1237–1239. (h) Turk, J. A.; Visbal, G. S.; Lipton, M. A. *J. Org. Chem.* **2003**, *68*, 7841–7844.
(18) Ratnayake, A. S.; Bugni, T. S.; Feng, X.; Harper, M. K.; Skalicky, J. J.; Mohammed, K. A.; Andjelic, C. D.; Barrows, L. R.; Ireland, C. M *J. Nat. Prod.* **2006**, *69*, 1582–1586.
(19) Pisera, A.; Lévi, C. In *Systema Porifera: A Guide to the Classification of Sponges*; Hooper, J. N. A., van Soest, R. W. M., Eds.; Kluwer Academic/Plenum Publishers: New York, 2002; pp 327–337.
(20) Louis, J. L.; Nesheiwat, I.; Chang, L. C.; Clore, G. M.; Bewley, C. A. *J. Biol. Chem.* **2003**, *278*, 20278–20285.
(21) Mascola, J. R.; D'Souza, P.; Gilbert, P.; Hahn, B. H.; Haigwood, N. L.; Morris, L.; Petropoulos, C. J.; Polonis, V. R.; Sarzotti, M.; Montefiori, D. C. *J. Virol.* **2005**, *79*, 10103–10107.

NP070306K